Identification and Characterization of chCR2, a Protein That Binds Chicken Complement Component 3d

Huan Jin,* ZiMeng Kong,† Bo Jiang,*,‡ Min Tu,* Jian Xu,*,‡ Jing Cheng,*,‡ Wenxiao Liu,*,‡ Zhenhua Zhang,* and Yongqing Li*,‡

Complement receptor type 2 (CR2) is an important membrane molecule expressed on B cells and follicular dendritic cells. Human CR2 has been shown to play a critical role in bridging the innate complement-mediated immune response with adaptive immunity by binding complement component 3d (C3d). However, the chicken CR2 (chCR2) gene has not been identified or characterized. In this study, unannotated genes that contain short consensus repeat (SCR) domains were analyzed based on RNA sequencing data for chicken bursa lymphocytes, and a gene with >80% homology to CR2 from other bird species was obtained. The gene consisted of 370 aa and was much smaller than the human CR2 gene because 10–11 SCRs were missing. The gene was then demonstrated as a chCR2 that exhibited high binding activity to chicken C3d. Further studies revealed that chCR2 interacts with chicken C3d through a binding site in its SCR1–4 region. An anti-chCR2 mAb that recognizes the epitope ^{258}CKEISCVFPEVQ^{269} was prepared. Based on the anti-chCR2 mAb, the flow cytometry and confocal laser scanning microscopy experiments confirmed that chCR2 was expressed on the surface of bursal B lymphocytes and DT40 cells. Immunohistochemistry and quantitative PCR analyses further indicated that chCR2 is predominantly expressed in the spleen, bursa, and thymus, as well as in PBLs. Additionally, the expression of chCR2 varied according to the infectious bursal disease virus infection status. Collectively, this study identified and characterized chCR2 as a distinct immunological marker in chicken B cells. ***The Journal of Immunology*****, 2023, 210: 1408–1418.**

The complement system is an ancient and complex immune defense system. It was first discovered in the late 19th century as a heat-sensitive factor in fresh serum (1). It is found in humans and other animals and represents one of the most important components of the innate immune system response to foreign invasion and consists of a series of heat-sensitive proteins with enzyme activity (2). It is composed of ~40 different proteins, including inherent components (C1q, mannan-binding lectin, C2, C4, B, D, C3, and C5–9), regulatory factors (C1 inhibitors, I factors, H factors, and C4-binding proteins), and complement receptors (CRs; CR1–5 and C2aR), which mediate a series of precise protein interactions to form immune complexes that quickly clear foreign invaders (3, 4). Activation of the complement system occurs mainly through the classical, mannan-binding lectin or alternative pathways to consequently form the membrane attack complex, which dissolves and destroys target cells. In addition to its involvement in inflammation, the complement system also enhances the adaptive immune response by releasing cell lysates and interacting with surface receptors on various cells. These complex interactions between complement-activated products and cell surface receptors regulate the response of B and T cells (5–10).

CRs are the targets of various active compounds during complement activation and they are localized on the surface of a variety of host cells. Upon ligand binding, a variety of biological effects can be induced. Among CRs, CR type 2 (CR2) is a transmembrane glycoprotein mainly localized on the surface of mature B cells and follicular dendritic cells (11–13). It is a member of the regulators of complement activation (RCA) gene cluster family. Members of this family have similar complex control protein (CCP) domains, also known as short consensus repeats (SCRs) (14–16). CR2 ligands include iC3b, C3dg, IFN-α, CD23 (FcεRII), and EBV surface glycoprotein gp350/220 (11, 17–19). The main physiological ligand of CR2 is the 35-kDa protein C3d. Through x-ray crystallography and other methods, the C3d binding region was determined to be located in SCR1–2 of CR2 (16, 20, 21). The interaction between CR2 and C3d plays an important role in the activation of B cells and the initiation of the immune response.

*Institute of Animal Husbandry and Veterinary Medicine, Beijing Academy of Agricultural and Forestry Sciences, Beijing, People's Republic of China; †College of Veterinary Medicine, China Agricultural University, Beijing, People's Republic of China; and ‡Beijing Key Laboratory for Prevention and Control of Infectious Diseases in Livestock and Poultry, Beijing Academy of Agricultural and Forestry Sciences, Beijing, People's Republic of China

ORCIDs: 0000-0002-5595-2039 (H.J.); 0000-0003-3944-6598 (Z.K.); 0000-0001-9459-5030 (B.J.).

Received for publication June 14, 2022. Accepted for publication February 8, 2023.

This work was supported by the National Natural Science Foundation of China Grants 31672588 and 32202793, Special Program on Science and Technology Innovation Capacity Building of BAAFS Grant KJCX20220422, and by Youth Fund of BAAFS Grant QNJJ202111.

H.J. performed the experiments and wrote the manuscript; Z.K., B.J., and M.T. performed the experiments; Y.L. and Z.Z. designed the study and wrote and revised the manuscript; and J.X., J.C., and W.L. analyzed the data. All authors contributed to the article and approved the submitted version.

The chCR2 gene sequence presented in this article has been submitted to the GenBank (https://www.ncbi.nlm.nih.gov/nuccore/MW054860.1/) under accession number MW054860.1.

Address correspondence and reprint requests to Prof. Yongqing Li and Prof. Zhenhua Zhang, Institute of Animal Husbandry and Veterinary Medicine, Beijing Academy of Agricultural and Forestry Sciences, Beijing 100097, People's Republic of China. E-mail addresses: liyongqing@baafs.net.cn (Y.L.) and zhangzhenhua@baafs.net.cn (Z.Z.)

The online version of this article contains supplemental material.

Abbreviations used in this article: CCP, complex control protein; C3d, complement component 3d; chCR2, chicken CR2; CLSM, confocal laser scanning microscopy; co-IP, coimmunoprecipitation; CR, complement receptor; CR2, CR type 2; 3D, three-dimensional; DAB, diaminobenzidine; FCM, flow cytometry; IBDV, infectious bursal disease virus; IFA, immunofluorescence assay; IHC, immunohistochemistry; MDV, Marek's disease virus; RCA, regulators of complement activation; RT, room temperature; SCR, short consensus repeat; SPF, specific pathogen-free; SPR, surface plasmon resonance; WB, Western blotting.

Human CR2 is composed of an extracellular region of 951 or 1010 aa (15–16 repetitive SCR/CCP modules), a 28-aa transmembrane region, and a 34-aa cytoplasmic tail (13, 22, 23). Each SCR segment has four conserved cysteine residues (module boundaries are defined as Cys-I and Cys-IV), one tryptophan residue, and disulfide bonds formed by Cys-I/Cys-III and Cys-II/Cys-IV (11). Moreover, CR2 has been reported to be expressed on mature B cells but not on precursor or immature B cells. This is because CpG island methylation on the CR2 promoter represses its transcription. Its expression in mature B cells is often accompanied by the loss of CpG methylation (24, 25). CR2 binds noncovalently to CD19, CD81, and Leu^{13} to form a receptor complex on the B cell surface that cross-links with the BCR and can reduce the amount of Ag required for B cell activation (26, 27). When a large number of Ags are present, the signal transduction caused by the cross-linking of this B cell coreceptor complex with BCR is not clear because the cross-linking between BCR complexes is sufficient to produce a considerable reaction. When the amount of Ag is insufficient, such as during initial exposure to infectious agents, Ags covalently linked to C3d bind with CR2 on the surface of B cells, causing Ig α/β heterodimer and CD19 intracellular tyrosine-activating motif phosphorylation and recruitment of other signal transducers such as SYK, VAV, and PI3K. This eventually promotes B cell activation by reducing its threshold by 10- to 1000-fold (28–33). Therefore, the interaction of CR2 with C3d plays an optimal role in stimulating the B cell response to Ags.

Although the functional mechanism of CR2 is relatively well elucidated in humans, the chicken CR2 (chCR2) has not been previously identified or characterized, which could hinder the fundamental understanding of the avian immune system. Recently, we investigated the transcriptional profile of Marek's disease virus (MDV)–mediated immune responses in chicken bursa lymphocytes by using high-throughput RNA sequencing. Our results demonstrate that significant differences occur in the functions of B cells that support the early cytolytic replication of MDV (34). However, we also noticed that the expression of certain unknown genes changes during MDV infection. Therefore, in this study, we further analyzed the data and found one unannotated gene (MW054860) that presented >80% homology with bird CR2 genes published in GenBank. Then, the gene was identified and characterized as chCR2, which is a receptor of chC3d and a specific immunological marker in chicken B cells. In addition, the chCR2 protein consisted of 370 aa, which was much smaller than the human CR2 due to the lack of 10–11 SCRs. Additionally, an mAb against chCR2 was developed. Taken together, these results will help to fill the gaps in poultry immunology research and provide tools for studying the avian immune system.

Materials and Methods

Animals and experimental design

Female specific pathogen-free (SPF) BALB/c mice aged 7–8 wk used to prepare the mouse monoclonal anti-chCR2 Ab were maintained at Beijing Boehringer Ingelheim Vital Biotechnology (Beijing, China). Mice were raised under a normal light/dark cycle and provided with standard laboratory food and water ad libitum.

Chicks and chickens were acquired from SPF white leghorn flocks, maintained at Beijing Boehringer Ingelheim Vital Biotechnology.

Twenty SPF chicks (mixed-sex, 1-d-old chicks) were reared in the same cage. Chicks were provided with feed and drinking water ad libitum. Chicks were euthanized humanely, and tissue samples were collected from five birds at regular intervals (7, 14, 21, and 28 d postinfection).

Twenty SPF chickens (mixed-sex, 3-wk-old chickens) were divided randomly into four groups (mock, infectious bursal disease virus [IBDV] infection control, low-dose vaccine, and high-dose vaccine) and each group was reared in separate cages. Each chicken in the vaccine groups was vaccinated i.m. with IBDV inactivated vaccine (0.02 ml/0.5 ml). Mock-treated chickens in the control group were vaccinated with PBS (0.5 ml). At 4 wk postvaccination, each bird from the vaccine groups and IBDV infection control groups was challenged via the intraocular–nasal route with 0.2 ml of the very virulent IBDV strain BJQ902 (mean bird infectious dose = $10^{6.7}$/0.2 ml). All chickens were humanely euthanized and bursa samples were collected from five birds in each group at 72 h postinfection.

Cells

DF-1 cells (fibroblast cells, derived from an East Lansing Line chicken embryo, which was spontaneously immortalized), HEK 293 cells (kidney cells, derived from human embryonic kidney cells grown in tissue culture), and SP2/0 cells (myeloma cells, derived from mouse myeloma) were cultured in DMEM (Life Technologies, Waltham, MA) supplemented with 10% FBS (Life Technologies) and maintained at 37°C in a humidified 5% CO_2 incubator. DT40 cells (B lymphocyte line, derived from Hy-Line SC chicken bursa B cells, which were induced by avian leukosis virus) were maintained in DMEM supplemented with 10% FBS and 5% chicken serum (Life Technologies). B lymphocytes (34) were maintained in RPMI 1640 supplemented with 10% FBS. HEK 293F cells (suspension cells, derived from the 293 cells line) were cultured in OPM-293 CD05 medium (OPM Biosciences, Shanghai, China).

Abs used

Abs for pull-down, immunoprecipitation, immunofluorescence assay (IFA), flow cytometry (FCM), immunohistochemistry (IHC), ELISA, and Western blotting (WB) were as follows: monoclonal and polyclonal anti–HA/β-actin, anti-Myc, anti-GFP, anti-His Abs (Sigma-Aldrich, St. Louis, MO); monoclonal anti-Na/K ATPase of rabbit (Abmart, Shanghai, China); mouse monoclonal anti-chCR2 Ab was prepared as described in this study; HRP-conjugated goat anti-rabbit IgG and HRP-conjugated goat anti-mouse IgG Abs (Sigma-Aldrich); Alexa Fluor 488–conjugated goat anti-mouse IgG (H+L) $F(ab')_2$ fragment and Alexa Fluor 568-conjugated goat anti-rabbit IgG (H+L) $F(ab')_2$ fragment Abs (Molecular Probes, Waltham, MA); and Alexa Fluor 647–conjugated mouse anti-chicken Bu-1 Ab (Southern Biotech, Birmingham, AL).

Plasmid construction

The coding region of chCR2 was amplified from the total RNA of chicken bursa lymphocytes using PCR with primers designed based on sequences available in GenBank (AJ720954.1, *Gallus gallus* mRNA for hypothetical protein, clone 31a4), and reverse transcription was performed using the HiScript III first-strand cDNA synthesis kit (+gDNA wiper) (Vazyme, Nanjing, China) to generate cDNAs. DNA was amplified using KOD FX Neo (Toyobo, Osaka, Japan), and the products were extracted using a FastPure gel DNA extraction mini kit (Vazyme) according to the manufacturer's protocols. This sequence and deletions derived from it were cloned into the expression plasmids pCMV-HA, pGEX-6P-1, and pTT5 with a 6*His-tag to generate pCMV-HA-chCR2, pCMV-HA-chCR2-ΔTM, pGEX-6P-1-chCR2-ΔTM, and pTT5-chCR2-His.The chCR2 truncation sequences, that is, chCR2-SCR1, chCR2-SCR1–2, chCR2-SCR1–3, chCR2-SCR1–4, chCR2-SCR2–5, chCR2-SCR3–5, chCR2-SCR4–5, and chCR2-SCR5, were cloned into the plasmid pEGFP-N2. chC3d was cloned from the chicken genome into the expression plasmid pCMV-Myc and pTT5 with a 6*His-tag to generate pCMV-Myc-chC3d and pTT5-chC3d-His, respectively.

Expression and purification of chCR2 and chC3d protein

The GST-chCR2 fusion protein was obtained by using a prokaryotic expression system. The expression products were then purified by using the Glutathione Sepharose 4 Fast Flow purification system. The His-chCR2 and His-chC3d proteins were obtained by using a eukaryotic expression system. pTT5-chCR2-His and pTT5-chC3d-His plasmids were transfected into the HEK 293F cells, respectively. The expression products in the cultured medium were harvested and purified using the Ni purification system.

Preparation of the anti-chCR2 mouse mAb

The chCR2-specific mAbs were generated according to established protocols with slight modifications (35). Briefly, 6-wk-old BALB/c mice were primed s.c. with 100 μg of recombinant his-chCR2 protein emulsified with Freund's complete adjuvant (Sigma-Aldrich) in an equal volume. The mice were boosted twice at 3-wk intervals with the same dose of his-chCR2 in an equal volume of Freund's incomplete adjuvant (Sigma-Aldrich). Three days after the final i.p. injection booster with his-chCR2 protein only, the mice were euthanized and spleen cells were collected and fused with SP2/0 myeloma cells using polyethylene glycol (PEG1450) (Sigma-Aldrich). The fused cells were seeded in 96-well plates and cultured in DMEM containing

hypoxanthine-aminopterin-thymidine (HAT) (Sigma-Aldrich) and 20% FBS. mAbs against chCR2 were screened out from the hybridoma cell supernatant by indirect ELISA using his-chCR2 as a positive selection Ag and his-irrelevant protein as the negative selection Ag. Positive hybridomas were subcloned over three rounds by limiting dilution, and the ascites fluid was produced and purified following routine procedures (35).

Pull-down and WB assays

Direct interactions between chC3d and chCR2 were analyzed using a pull-down assay. GST-chCR2-ΔTM proteins were expressed in *Escherichia coli* and His-chC3d proteins were expressed in 293F cells. Proteins were precipitated with anti-GST magnetic beads (Thermo Fisher Scientific, Waltham, MA). Proteins were separated by SDS-PAGE and assessed by Coomassie Brilliant Blue staining or WB after transfer onto a polyvinylidene difluoride membrane (Millipore, Burlington, MA). Subsequently, the membranes were washed with PBS with 0.5% Tween 20 (PBST), probed with appropriate primary Abs (anti-GST and anti-His Abs at 1:5,000 dilution), and then incubated with HRP-conjugated goat anti-mouse IgG or HRP-conjugated goat anti-rabbit IgG (1:10,000 dilution). Finally, the membranes were washed again and then visualized using the ECL WB system (Thermo Fisher Scientific).

Coimmunoprecipitation assay

Interactions between chC3d and chCR2 or chC3d and truncated chCR2 were analyzed using coimmunoprecipitation (co-IP) and WB. At 24 h after transfection, proteins were extracted from HEK 293 cells that were cotransfected with pCMV-Myc-chC3d and pCMV-HA-chCR2-ΔTM or pCMV-Myc-chC3d and truncated chCR2, and then the proteins were precipitated with anti-HA beads (Thermo Fisher Scientific). The protein samples isolated from the beads were separated by 12% SDS-PAGE, transferred onto a polyvinylidene difluoride membrane (Millipore), and probed with appropriate primary Abs (anti-HA, anti-GFP, and anti-Myc Abs at 1:5000 dilution). Subsequently, the membranes were washed with 0.05% PBST and incubated with HRP-conjugated goat anti-mouse IgG or goat anti-rabbit IgG (1:10,000 dilution). Membranes were washed again and then visualized using the ECL WB system (Thermo Fisher Scientific).

IFA and confocal laser scanning microscopy

DF-1 cells were grown on coverslips in six-well plates to 50–70% confluency, then cotransfected with plasmids expressing chC3d and either chCR2, truncated chCR2, or empty plasmid. At 24 h posttransfection, the cells were fixed with 3.7% paraformaldehyde for 10 min at room temperature (RT), permeabilized for 10 min with PBS containing 0.1% Triton X-100 and 2% BSA, and blocked with 2% BSA/PBS for 30 min. The cells were then incubated with the appropriate primary Abs (pCMV-HA-chCR2 and pCMV-HA-chCR2-ΔTM were stained with a mouse monoclonal anti-HA Ab at 1:1000 dilution), and pCMV-Myc-chC3d was stained with a rabbit polyclonal anti–c-Myc Ab at 1:1000 dilution) at RT for 1 h in a humid chamber. After washing three times with PBS for 5 min each, cells were incubated with appropriate secondary Abs (Alexa Fluor 488–conjugated goat anti-mouse IgG and Alexa Fluor 568–conjugated goat anti-rabbit IgG at 1:1000 dilution) for another 1 h at RT in a humid chamber and washed. Finally, nuclear DNA was stained with DAPI (Sigma-Aldrich), and images were scanned under an Olympus (Tokyo, Japan) confocal microscope.

DT40 cells were grown on a 12-mm Nunc glass base dish (Thermo Fisher Scientific) to 50–70% confluency. After natural drying, the cells were fixed with 3.7% paraformaldehyde for 10 min at RT, permeabilized for 10 min with PBS containing 0.1% Triton X-100 and 2% BSA, and blocked with 2% BSA/PBS for 30 min. The cells were then incubated with the appropriate primary Abs (anti-Na/K ATPase Ab at 1:200 dilution, and the anti-chCR2 mAb at 1:500 dilution) at RT for 1 h in a humid chamber. After washing three times with PBS for 5 min each, the cells were incubated with the secondary Abs Alexa Fluor 488–conjugated goat anti-mouse IgG and Alexa Fluor 568–conjugated goat anti-rabbit IgG (1:1000 dilution) for another 1 h at RT in a humid chamber and washed. Finally, nuclear DNA was stained with DAPI (Sigma-Aldrich), and images were scanned under an Olympus (Tokyo, Japan) confocal microscope.

Surface plasmon resonance measurements

Affinity analysis was performed using a Biacore T100 instrument (GE Healthcare Life Sciences) at the Institute of Biophysics, Chinese Academy of Science. All of the experiments were performed at RT in PBS containing 0.05% Tween 20 (pH 7.4). chCR2 protein was directly immobilized on the CM5 chip (series S sensor chip CM5, Cytiva) using an amine coupling kit (Cytiva). Before immobilization, the CM5 sensor surface was activated using a mixture of 400 mM 1-ethyl-3-(3-dimethylaminopropyl) carbodiimide (EDC) and 100 mM *N*-hydroxysuccinimide (NHS). Then, 20 μg/ml chCR2 in immobilization buffer (10 mM NaAc [pH 4.5]) was injected into the Fc3 sample channel at a flow rate of 10 μl/min. The amount of ligand immobilized was ~4800 resonance units. The chip was blocked with 1.0 M ethanolamine-HCl (pH 8.5) (Cytiva) at a flow rate of 10 μl/min for 420 s. The reference Fc1 channel was used as a blank control, which underwent similar procedures but without injecting the ligand. The chC3d protein was serially diluted with the running buffer to generate concentrations of 5, 2.5, 2.5, 1.25, 0.625, 0.3125, and 0.15625 μM. Different concentrations of chC3d proteins were then injected into Fc3-Fc1 channels at a flow rate of 30 μl/min, contact time of 60 s, and dissociation time of 90 s. After each cycle of interaction analysis, the analyte injection, the association and dissociation processes were performed in the running buffer. Data were analyzed on the Biacore T100 computer using Biacore T100 evaluation software and the 1:1 binding model.

RNA extraction, cDNA synthesis, and quantitative real-time PCR

Total RNA was extracted from each tissue sample using TRIzol reagent (Invitrogen, Waltham, MA) and treated with RNase-free DNase I (Tiangen, Beijing, China) to remove possible contaminating DNA. Following isolation, the RNA concentration in the samples was determined, and 1000 ng of RNA was reverse transcribed to cDNA using the FastKing RT (reverse transcription) kit (with gDNase). For each experiment, a non-template reaction was included as a negative control. The primers for the detection of chCR2 are forward, 5′-ATGGCCCAGTGCAAAGCTGAC-3′ and reverse, 5′-CTAGTCCAGAGAGGTTTTGTA-3′. The quantitative PCR cycling conditions were as follows: 2 min at 95°C followed by 40 cycles of 15 s at 95°C and then 1 min at 60°C, and a dissociation curve (15 s at 95°C, 1 min at 60°C, 15 s at 95°C, and 15 s at 60°C). All target gene expression levels were normalized to that of the GAPDH gene. All samples were subjected to RNA extraction three times and tested in triplicate.

FCM analysis

FCM was used to analyze chCR2 expression in chicken B cells. After resuscitation of bursa lymphocytes and DT40 cells, cells were divided into four groups with 10^6 cells each. Cells were washed once with PBS, centrifuged, and the supernatant was discarded. Next, 200 μl of precooled 4% paraformaldehyde was added and cells were fixed for 6–8 min on a shaker at RT. Samples were then centrifuged, paraformaldehyde was discarded, and cells were washed three times with PBS for 5 min each. Next, 5% mouse polyclonal IgG Abs were added, and samples were incubated at RT on a shaker for 30 min. Samples were then centrifuged to discard the supernatant and washed three times with PBS for 5 min each. The fluorescently labeled Alexa Fluor 647–conjugated mouse anti-chicken Bu-1 Ab (0.1μg/10^6cells) or anti-chCR2 mAb (1:500 dilution) was added at RT, followed by the appropriate fluorescently labeled secondary Ab (Alexa Fluor 488–conjugated goat anti-mouse IgG, 1:1000 dilution). Samples were incubated on a shaker at RT for 15 min, centrifuged to discard the supernatant, gently absorbed, and then washed three times with PBS. Finally, samples were filtered through a cell sieve and analyzed by FCM. Data were collected on an Agilent ACEA NovoCyte 2060R flow cytometer (Agilent) and analyzed with FlowJo software (Tree Star, Ashland, OR).

IHC staining

IHC staining of sections of spleen, bursa, thymus, lung, and liver tissues from chickens was performed using a Dako (Tokyo, Japan) kit with mouse monoclonal anti-chCR2 Abs (1:500 dilution). Tissues were fixed in formalin, embedded in paraffin, and then sectioned. The tissue sections were deparaffinized, rinsed with running water for 5 min, treated with freshly prepared 3% hydrogen peroxide aqueous solution for 30 min at RT, washed with single distilled water for 5 min, and then washed twice with PBS for 5 min each. The slides were steam repaired using the repair solution (DM828), maintained at 95–100°C for 30 min, and then cooled naturally. Slides were washed three times with the elution buffer (K8007) for 5 min each. The remaining elution buffer was shaken off and an IHC pen was used to enclose the tissue on the slides before incubation with the blocking solution (SM801) in a humidified box for 1 h at 37°C. Next, slides were incubated with anti-chCR2 mAb at 4°C for 12 h. After three 5-min incubations in elution buffer, slides were incubated with the HRP-labeled secondary Ab (SM802) for 45 min at 37°C, followed by washing three times with elution buffer for 5 min each. Slides were colored with the diaminobenzidine (DAB) chromogenic solution (DAB condensed chromogen [DM827] diluted with DAB dilution buffer [SM803] and mixed well), and color development was controlled under a microscope. The slides were counterstained with hematoxylin for 2–4 min, then rinsed with tap water for 10 min, and subsequently dehydrated and clarified with 80% alcohol (2 min), 95% alcohol I (2 min), 100% alcohol I (2 min), 100% alcohol II (2 min), xylene I (15 min), and xylene II (15 min). The slides were sealed with neutral resin and dried naturally.

Data and statistical analysis

All tests were performed in triplicate in accordance with the biostatistical requirements. Graphs were generated using GraphPad Prism 5.0. ExPASy (https://web.expasy.org/protparam/), SMART (http://smart.embl-heidelberg.de/smart/set_mode.cgi?NORMAL=1), and SWISS-MODEL (https://swissmodel.expasy.org/) were used for online analyses.

Ethics approval

All animal care procedures and experiments were approved by the Beijing Association for Science and Technology (approval ID SYXK [Beijing] 2019–0023) and were in compliance with the Beijing Laboratory Animal Welfare and Ethics guidelines issued by the Beijing Administration Committee of Laboratory Animals. All animal studies were also in accordance with the Beijing Academy of Agricultural and Forestry Sciences Animal Care and Use Committee guidelines (ID SYXK [Jing] 2017–0039) and were approved by the Animal Welfare Committee of the Beijing Academy of Agricultural and Forestry Sciences.

Results

Sequence determination and structural characteristics of chCR2

Previously, the transcriptomes of chicken bursa lymphocytes were obtained using high-throughput RNA sequencing (34). In this study, the novel transcripts and uncharacterized genes were analyzed and a chicken gene with >80% homology to CR2 from other bird species was identified, and it contained SCR domains consistent with typical RCA family members (Table I). In addition, the sequence of this gene was 99.73% consistent with the sequence of a hypothetical protein from chicken bursal lymphocytes (AJ720954.1) deposited in GenBank (Table I). Therefore, the coding gene designated as chCR2 was cloned separately from bursa lymphocytes and DT40 cells by RT-PCR with primers designed based on the GenBank sequence for AJ720954.1. The resulting 1113-bp PCR product was consistent with the expected size (Supplemental Fig. 1A). The chCR2 gene sequence was then submitted to GenBank (MW054860.1, https://www.ncbi.nlm.nih.gov/nuccore/MW054860.1/) and mapped to chromosome 26 of the chicken genome. A phylogenetic tree of mammalian and bird CR2 genes was generated by MEGA6 and showed that chCR2 was closely related to other birds including *Acanthisitta chloris*, *Melopsittacus undulatus*, and *Aquila chrysaetos canadensis*, but distantly related to mammals (Fig. 1A). The chCR2 domain predicted by SMART showed that chCR2 is composed of five CCP/SCR domains, a transmembrane domain, and a cytoplasmic tail typical of CR2 (Fig. 1B–D). A multiple sequence alignment of the five chCR2 SCR modules showed several highly conserved amino acid residues, including one glycine, one tryptophan, and three prolines, as well as two disulfide bonds formed between the four invariant cysteine residues, consistent with human CR2, suggesting that functional significance developed during evolution (Fig. 1C).

Analysis of the tertiary structure revealed that the SCR domains of chCR2 were formed by repetitive β-folding, which is typical of members of the RCA gene cluster family (Fig. 1E). Complement factor H (PDB: 5O35.1C), a member of the RCA protein family, was used as the template to analyze the three-dimensional (3D) structure of chCR2 and its truncated SCRs. The 3D models showed that CR type 1 (PDB: 1GKG.1.A) is the template for SCR1 and SCR3, complement decay-accelerating factor (PDB: 1H04.1.A and 2QZD.1.A) is the template for SCR2 and SCR4, respectively, and membrane cofactor protein (PDB: 3O8E.1.F) is the template of SCR5 (Fig. 1E).

Table I. Uncharacterized gene identified by RNA sequencing data

Gene ID	Identity (%)	Gene Description
ENSGALG00000030007 (AJ720954.1)	99.73	Sushi_SCR_CCP_dom
ENSGALG00000023953	95.24	Sushi_SCR_CCP_dom
ENSGALG00000037721	94.74	Sushi_SCR_CCP_dom

These data indicate that chCR2 shares structural characteristics with other members of the RCA protein family.

chCR2 interacts with its physiological ligand chC3d

Because previous studies have not reported the interaction of the chCR2 receptor protein with its ligand chC3d, a pull-down assay (36) was performed to analyze the suspected interaction between the GST-chCR2 protein (Supplemental Fig. 2A, 2B) and His-chC3d protein (Supplemental Fig. 2C, 2E). As shown in Fig. 2A and 2B, pull-down with GST-chCR2 eluted His-chC3d. Furthermore, co-IP demonstrated that Myc-chC3d bound HA-chCR2 expressed in HEK293 cells (Fig. 2C).

Binding affinity is an important metric to evaluate the interaction strength between two biomolecules, such as receptors and ligands. In this study, surface plasmon resonance (SPR) was performed to analyze the protein–protein interaction affinity of chCR2 and chC3d. As determined by SPR, the His-chCR2 protein (Supplemental Fig. 2C, 2D) was directly immobilized on the CM5 chip, and different concentrations of the His-chC3d proteins were used as a ligand to flow over the His-chCR2 protein surface. Then, the K_D value was 1.37 μM (Fig. 2D). Therefore, the SPR results support the direct interaction of chCR2 with chC3d that was inferred based on the pull-down and co-IP.

In addition, we observed the interaction between chCR2 and chC3d by confocal laser scanning microscopy (CLSM) in DF-1 cells. Recombinant plasmids expressing HA-chCR2-ΔTM without the transmembrane domain (pCMV-HA-chCR2-ΔTM), and Myc-chC3d (pCMV-Myc-chC3d) were separately or cotransfected into DF-1 cells. As shown in Fig. 2E, Myc-chC3d and HA-chCR2-ΔTM were colocalized in the cytoplasm of DF-1 cells.

Identifying the chC3d-binding domain in chCR2

To investigate the interaction domain of chCR2 with chC3d, chCR2 truncation mutants were generated (Fig. 3A) and co-IP assays were performed. As shown in Fig. 3B–D, SCR1 through SCR1–4, and SCR2–5 through SCR4–5, but not SCR5, can interact with chC3d. These results were also supported by colocalization experiments (Fig. 3E, 3F) in DF-1 cells. Taken together, these results demonstrate that chCR2 interacts with chC3d through its SCR1–4 domains.

Identification of an anti-chCR2 mouse mAb

To explore the function of chCR2 and its distribution in chickens, an anti-chCR2 mAb was generated. IFA, WB, and ELISA analysis revealed that anti-chCR2 mAb reacted with chCR2 with higher specificity and affinity (Fig. 4A, 4B, Supplemental Fig. 3B, 3C). In particular, compared with gD protein of infectious bovine rhinotracheitis virus, VP2 protein of IBDV, chC3d protein, and GST protein, anti-chCR2 mAb can specifically bind chCR2 protein (Supplemental Fig. 3B). Additionally, anti-chCR2 mAb was IgG2b subtype with the κ-type L chain (Fig. 4C). To further determine the chCR2 epitope targeted by this anti-chCR2 mAb, a series of overlapping chCR2 truncation fusion proteins were analyzed by WB. The results showed that the mAb demonstrated highly specific binding to the epitope ^{258}CKEISCVFPEVQ^{269} located within SCR4–5 (Fig. 4D–G), indicating that the ^{258}CKEISCVFPEVQ^{269} epitope was recognized by this mAb. The purification, cross-reaction, and K_D are shown in Supplemental Fig. 3.

chCR2 is expressed on the surface of chicken B cells

Because human CR2 is a protein expressed on the surface of human B cells, we attempted to verify that chCR2 is a protein expressed on the surface of chicken B cells. B lymphocytes from bursa along with DT40 cells (a chicken B lymphoma cell line) were used for identifying the expression of chCR2. Meanwhile, the Bu-1 Ag is regarded as a surface marker of chicken B lymphoma cell, and the Bu-1–specific mAb could be used to identify and select B cells from

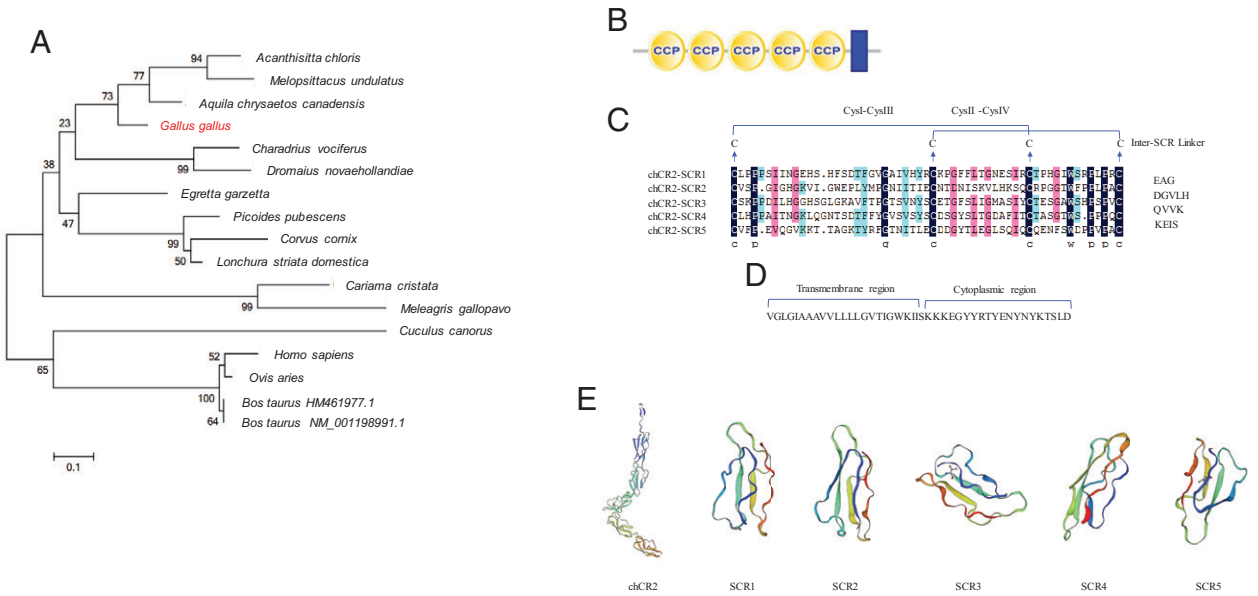

FIGURE 1. Sequence determination and structural characteristics of chCR2. (**A**) CR2 phylogenetic tree. (**B**) Schematic representation of chCR2. (**C**) Multiple sequence alignment of the SCR modules of chCR2 (module boundaries are defined as Cys-I and Cys-III, Cys-II and Cys-IV). Disulfide bonds formed between the conserved cysteines are indicated by lines. Also indicated are residues localized within the linker regions (ranging from 3 to 5 aa in length) that connect each SCR domain and the signal peptide with the SCR. (**D**) Amino acid sequence of the chCR2 transmembrane and cytoplasmic regions. (**E**) Predicted structure of the chCR2 SCR domains.

different chicken tissues, such as bursa, spleen, and PBLs (37, 38). Therefore, we employed FCM to compare the ratios of chCR2 in the bursa B cells and DT40 cell lines based on mAbs against Bu-1 and chCR2. The results showed that double-positive (chCR2-positive and Bu-1−positive) bursa lymphocytes and DT40 cells accounted for 80.62 and 98.04%, respectively (Fig. 5A, 5B). These data indicate that chCR2 is mainly expressed in chicken B cells. Moreover, CLSM showed that chCR2 can be localized on the cell membrane and colocalized with Na,K-ATPase, which is a marker of the plasma membrane on the membrane of DT40 cells (Fig. 5C). These results demonstrate that chCR2 is expressed on the surface of chicken B cells.

Distribution of chCR2 in different tissues

To understand the distribution of chCR2 in vivo, quantitative RT-PCR was performed to measure mRNA expression levels in different tissues and at different time points. The results showed that chCR2 was abundantly expressed in immune organs, such as the spleen, bursa, thymus, and PBLs but mostly not in nonimmune organs, such as the brain and liver (Fig. 6A–D). IHC was performed to map the distribution of chCR2 in chicken cells, and it showed that chCR2 was mainly detected in cells of the spleen, bursa, thymus, and lung relative to those of the liver (Fig. 6E) and other nonimmune organs, such as the heart, brain, and kidneys (data not shown). Furthermore, B cells are the primary target for IBDV in the bursa. Thus, to determine whether chCR2 expression was affected by viral infection, we proceeded to analyze the expression levels of chCR2 in bursa (Fig. 6F) and DT40 cells (Fig. 6G) infected with IBDV. Interestingly, compared with the control group, the expression level of chCR2 in bursa cells was increased postinfection with IBDV but decreased by immunization with the IBDV-inactivated

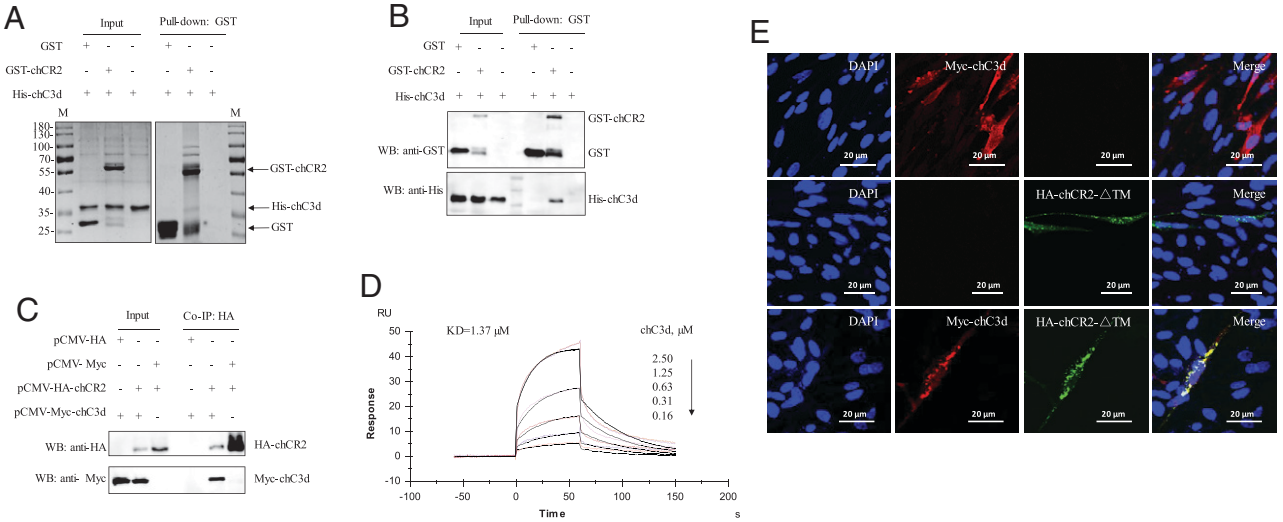

FIGURE 2. Interactions between chCR2 and chC3d. Interactions between chCR2 and chC3d were analyzed using a pull-down assay. (**A**) Coomassie stain. (**B**) WB. (**C**) Interaction of chCR2 with chC3d confirmed using a co-IP assay. (**D**) Measurement of the K_D for chCR2 and chC3d by SPR technology. (**E**) Colocalization analysis of chC3d with chCR2-ΔTM in DF-1 cells. In (A)–(E), data are representative of two independent experiments.

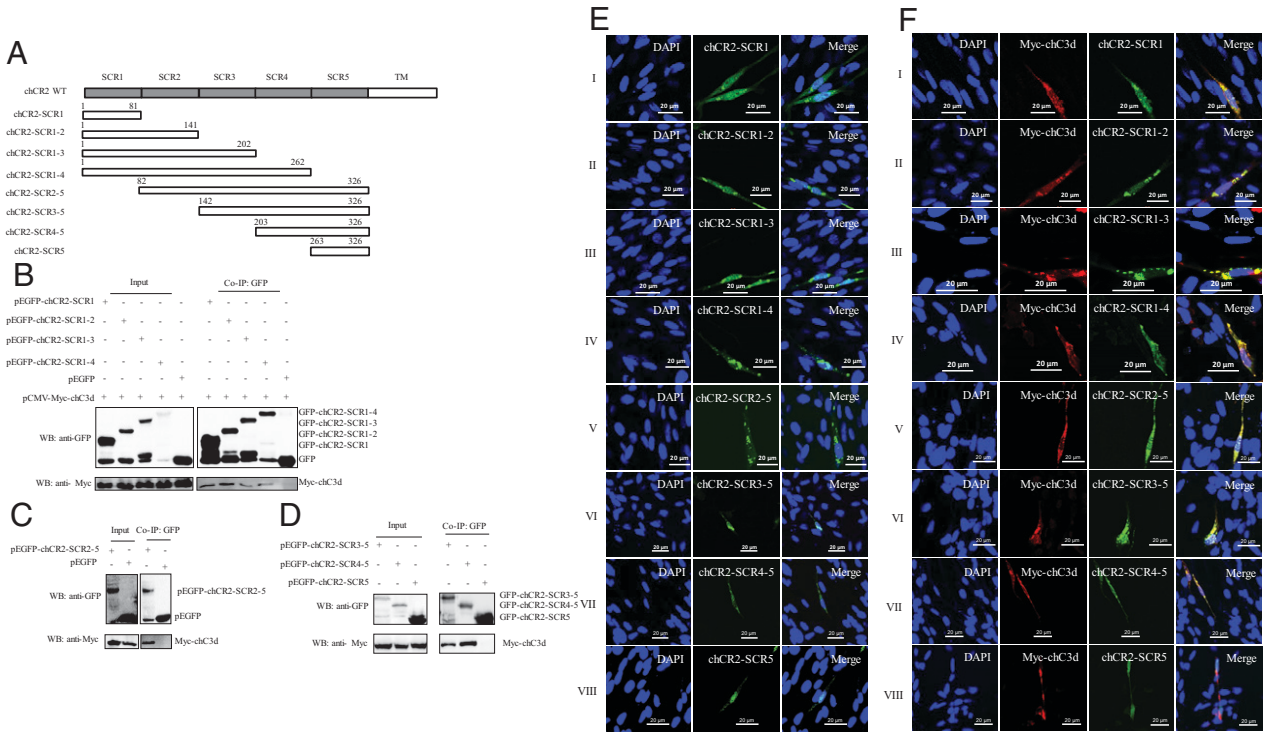

FIGURE 3. Determination of the binding domain of chCR2 with chC3d. (**A**) Schematic diagrams chCR2 truncation mutants (chCR2-SCR1, aa 1–81; chCR2-SCR1–2, aa 1–141; chCR2-SCR1–3, aa 1–202; chCR2-SCR1–4, aa 1–262; chCR2-SCR2–5, aa 82–326; chCR2-SCR3–5, aa 142–326; chCR2-SCR4–5, aa 203–326; and chCR2-SCR5, aa 263–326). (**B**) Co-IP with myc-chC3d and GFP-chCR2-SCR1, GFP-SCR1–2, GFP-SCR1–3, and GFP-SCR1–4. (**C**) Co-IP with myc-chC3d and GFP-chCR2-SCR2–5. (**D**) Co-IP with myc-chC3d and GFP-chCR2-SCR2–5, GFP-SCR3–5, or GFP-SCR4–5. (**E**) Localization of chCR2 truncation mutants in DF-1 cells measured by CLSM. (**F**) Colocalization of chCR2 truncation mutants with Myc-chC3d in DF-1 cells measured by CLSM. The truncated chCR2 (CR2-SCR1, chCR-SCR1–2, chCR2-SCR1–3, chCR2-SCR1–4, chCR2-SCR2–5, chCR2-SCR3–5, chCR2-SCR4–5, and chCR2-SCR5) was localized in the cytoplasm (E), and chCR2-SCR1–4 was colocalized with chC3d in the cytoplasm (F, **I–VIII**), whereas chCR2-SCR5 was not colocalized with chC3d (F, **VIII**). In (B)–(F), data are representative of two independent experiments.

vaccine in a dose-dependent manner, which was associated with the role of the vaccine, which inhibited the replication of the virus (Fig. 6F). Meanwhile, the WB analysis showed that IBDV infection (multiplicity of infection of 0.1) promoted the expression of chCR2 in DT40 cells at different time points (Fig. 6G). The copy number of IBDV mRNA is shown in Fig. 6H and 6I.

Discussion

Human CR2 (CD21) is a surface-associated glycoprotein that binds to a variety of endogenous ligands, including the complement component C3 fragments iC3b, C3d(g), and C3d; the low-affinity IgE receptor CD23; and the type I cytokine IFN-α (11, 14, 39). CR2 plays important roles in the immune system beyond its interactions with C3d by bridging the innate and acquired immune responses, amplifying cell signaling, and significantly reducing the amount of Ag required for B cell activation (11, 28). Variations or deletions of CR2 in humans and mice are associated with a variety of autoimmune and inflammatory conditions. Moreover, a number of infectious agents, including EBV, HIV, and prions, also bind to CR2 either directly or indirectly by means of C3d-targeted immune complexes (25). CR2 is also associated with the treatment of many diseases such as AIDS and cancer (40, 41). As a signal transduction molecule, CR2 plays an important role in enhancing antitumor immunity (42). The sequence of CR2 has been annotated in humans, mice, cattle, and other mammals, as well as some birds and aquatic animals (43, 44). However, the chicken immune system is very different from the mammalian immune system, and it is poorly understood due to the lack of corresponding findings and reagents. Therefore, identifying components of lymphocytes, such as chCR2, is invaluable for thoroughly investigating chicken immunological mechanisms and functions.

In this study, we successfully cloned the chCR2 gene from bursal lymphocytes. The chCR2 nucleotide sequence was 100% identical to one identified in the chicken B cell line DT40, implying that chCR2 could be expressed in chicken B lymphocytes. Phylogenetic analyses show that the chCR2 is orthologous to other bird CR2 sequences, but distantly related to those of humans and mammals (Fig. 1A), suggesting that the evolutionary relationship between mammalian and bird CR2 is significantly different. This is consistent with our previous investigations about the molecular evolutionary pattern of bird C3d, ligand of CR2 (45). Based on the predicted CR2 amino acid sequence, structural analyses indicated that chCR2 was composed of only five SCR domains (Fig. 1B) compared with human CR2, which contains 15–16 SCRs (11). Moreover, 3D modeling showed that chCR2 consists of five consecutive β-fold structure domains consistent with SCRs, a transmembrane region, and a cytoplasmic tail. Four disulfide-bound cysteine residues formed a (Cys-I/Cys-III)/(Cys-II/Cys-IV) motif, whereas 5 aa residues in conserved regions of chCR2 include one glycine, one tryptophan, and three prolines (Fig. 1C, 1D). These findings suggest evolutionary divergence of CR2 among different species, especially in birds. It likely reflects differences in the immune function of CR2 between birds and mammals.

Because CR2 mediates the immune response to pathogens and foreign Ags by binding with C3d, the immunological function of chCR2 is characterized by its interaction with chC3d. In the current study, to validate the biochemical function of chCR2, we conducted pull-down and co-IP assays to validate the interactions between

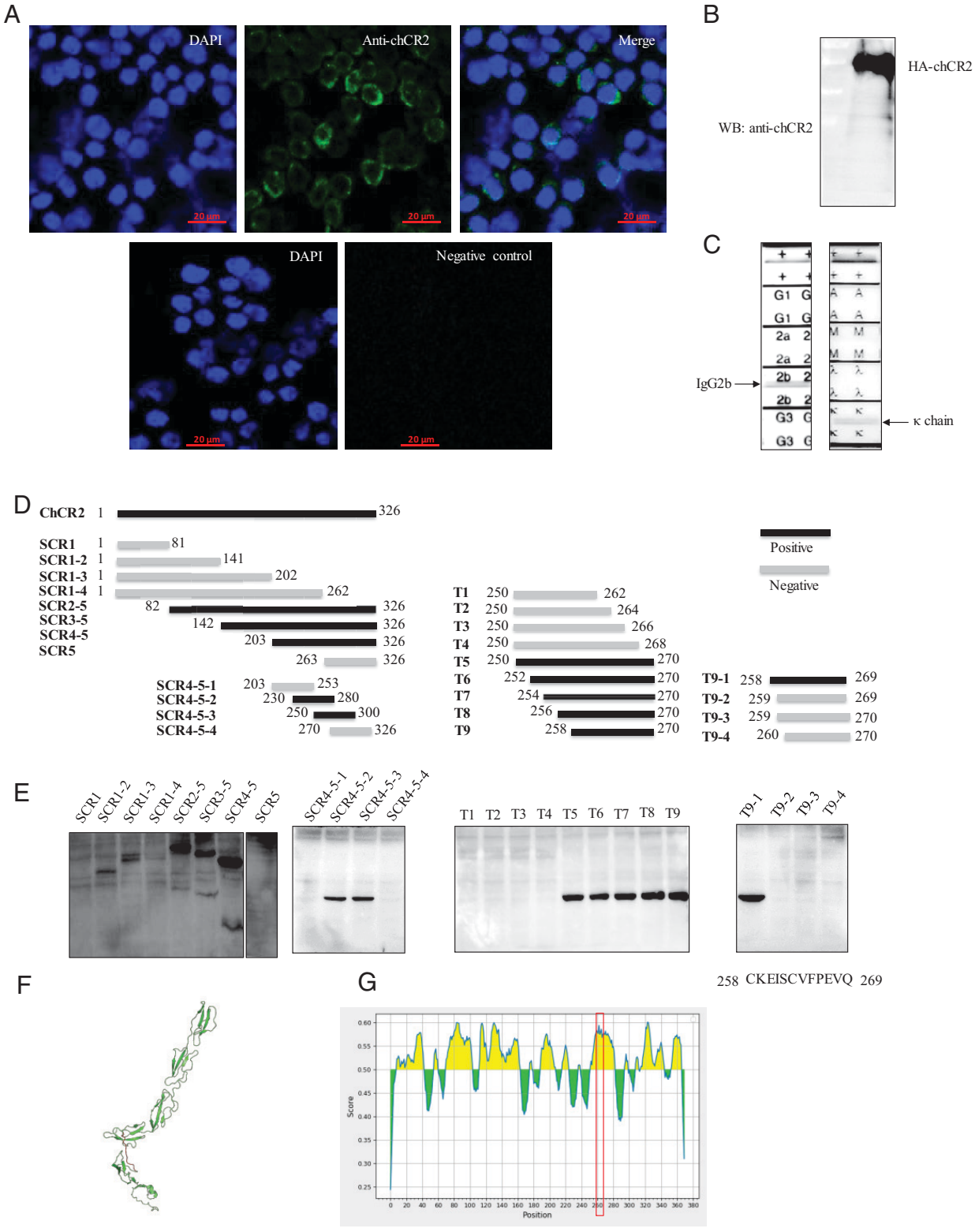

FIGURE 4. Preparation and identification of a mouse anti-chCR2 mouse mAb. Anti-chCR2 mouse mAb was prepared and the immunogenic epitope was identified. (**A** and **B**) The specificity of the mAb was analyzed by (A) IFA and (B) WB. (**C**) Anti-chCR2 mAb isotype. (**D**) Schematic design of overlapping chCR2 fragments and (**E**) the position of the epitope recognized by the chCR2 mAb at aa 258–269 identified by WB with the anti-chCR2 mAb. (**F**) Location of the identified chCR2 mAb epitope in a 3D structural model is highlighted in a loop. (**G**) Antigenic index of chCR2 protein was predicted using Bepipred Linear Epitope Prediction 2.0 with the epitope ^{258}CKEISCVFPEVQ^{269} highlighted (red box). In (A)–(C) and (E), data are representative of two independent experiments.

chCR2 and chC3d. We observed that chCR2 bound directly to chC3d in chicken cells (Fig. 2A–C). Moreover, when cotransfected, Myc-chC3d and HA-chCR2-ΔTM were colocalized in the cytoplasm of DF-1 cells (Fig. 2E), illustrating that chCR2 is a protein that recognizes chC3d. Subsequently, the SPR analysis confirmed the affinity of chCR2 and chC3d. The calculated K_D value of SPR is 1.37 μM,

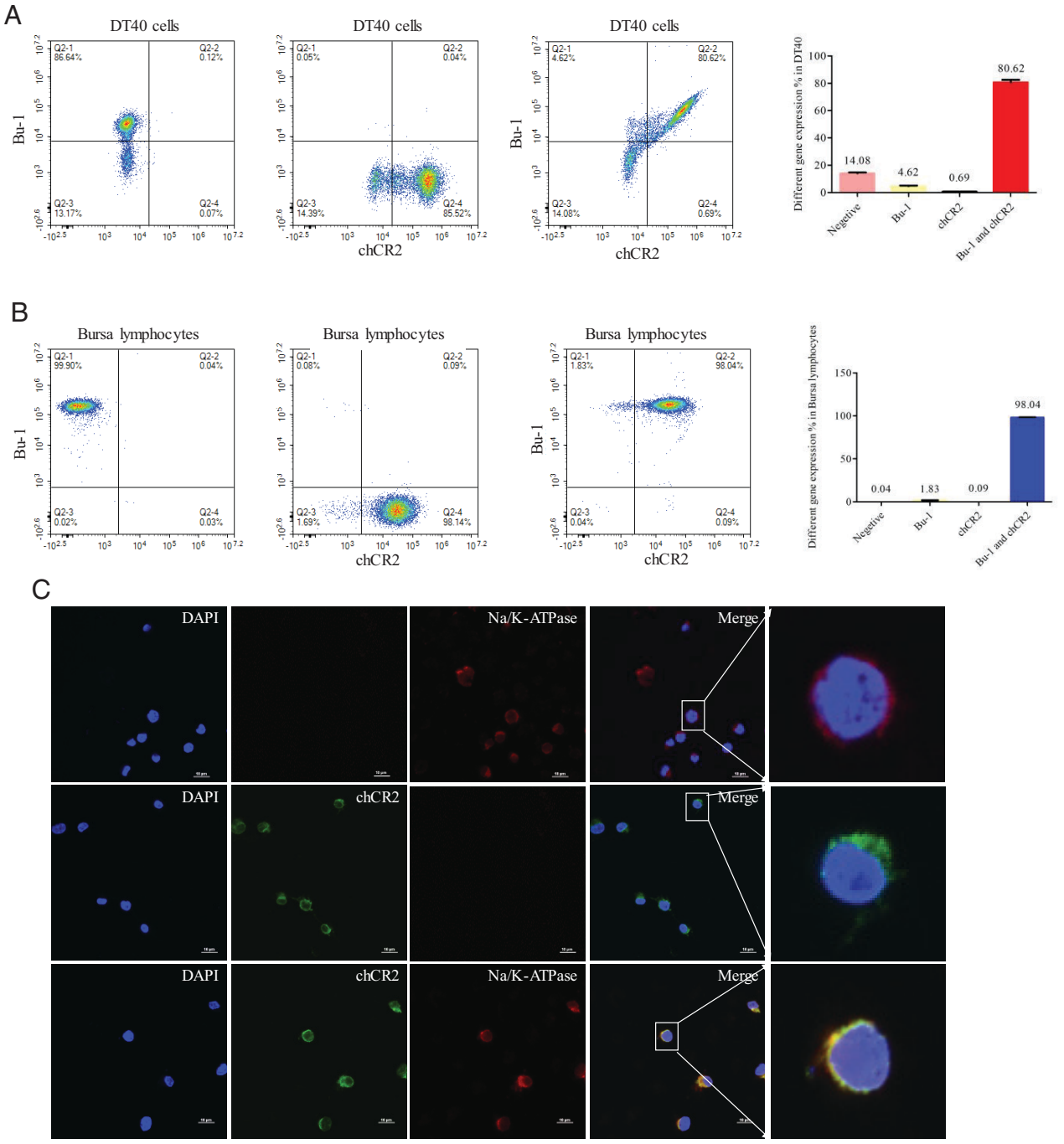

FIGURE 5. Expression of chCR2 on the surface chicken B cells. (**A** and **B**) In these experiments, cells were gated for Bu-1(B cell marker) and chCR2 alone or together, and then Bu-1– and chCR2-positive cells were observed. The results showed that (A) 80.62% of DT40 cells and (B) 98.04% of bursal lymphocytes expressed both Bu-1 and chCR2. The average, SD, range, median, and confidence interval were determined for the average of a total of three times for each study. (**C**) Colocalization of chCR2 with Na,K-ATPase in DT40 cells measured by CLSM. The chCR2 was colocalized with Na,K-ATPase on the cell membrane. Data are representative of two (C) or three (A and B) independent experiments.

which demonstrates that chCR2 has a high binding affinity to chC3d (Fig. 2D). The pull-down, co-IP, CLSM, and SPR data support the interaction of chCR2 and chC3d, thus highlighting that chC3d is an intriguing new ligand for chCR2.

The C3d binding domain in human CR2 is located mainly in the SCR1, SCR2, and linker domains (20, 21). In this study, we found that the chC3d-binding region of chCR2 included the SCR1–4 region, but not the SCR5 domain (Fig. 3). Notably, chCR2-SCR5 alone mainly accumulated in the nucleus, whereas the other truncations were distributed in the cytoplasm (Fig. 3E, VIII). This validates that four of five SCR domains in the N-terminal are required for the interaction of chCR2 with chC3d, and this interaction occurs predominantly in the cytoplasm. Interestingly, our previous structural analyses of bird C3d showed that the amino acids of bird C3d used to bind CR2 molecules were significantly different from those in mammalian C3d because an acidic pocket was observed on the concave surface of bird C3d, and it accounted for the binding CR2 (45). This finding hinted that, compared with the human CR2 and C3d, chCR2 may have different binding sites for interactions with the chC3d molecule.

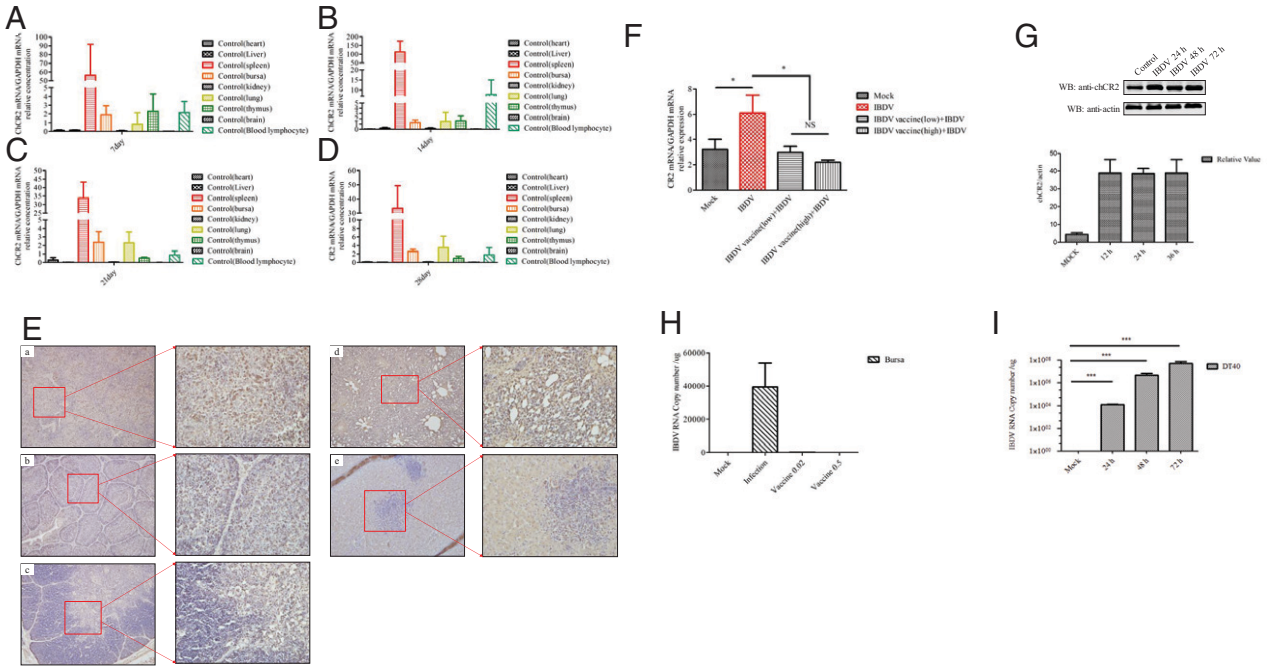

FIGURE 6. Expression of chCR2 in different chicken tissues. Distribution of chCR2 in different chicken tissues and at different time points. The expression of chCR2 was assessed using quantitative RT-PCR and IHC, and chCR2 was found to be mainly expressed in immune organs and PBLs. (**A**–**D**) Spleen, bursa, thymus, lung, heart, liver, kidney, and PBLs were collected on days (A) 7, (B) 14, (C) 20, and (D) 28 for quantitative RT-PCR analysis. (**E**) IHC analysis of spleen (**a**), bursa (**b**), thymus (**c**), lung (**d**), and liver (**e**) collected on day 28 (original magnification ×40). (**F** and **G**) Expression of chCR2 was detected in bursa and DT40 cells infected with IBDV. (**H**) Copy number of IBDV in different group in bursa. (**I**) Copy number of IBDV in different groups of DT40 cells at different time points. $*p < 0.05$, $***p < 0.001$ (two-way ANOVA followed by Bonferroni posttest). Data are representative of two (G) or three (A–F, H, and I) independent experiments.

To determine whether chCR2 is a receptor of chC3d on chicken B cells, the mAbs that recognize chCR2 must be identified. Therefore, we successfully generated a mAb against chCR2 and characterized it by IFA and WB (Fig. 4A, 4B), and this mAb could specifically react with chCR2 protein but not gD protein of infectious bovine rhinotracheitis virus, VP2 protein of IBDV, chC3d protein, and GST protein (Supplemental Fig. 3B), demonstrating that it has high specificity and affinity. In addition, epitope mapping showed that the sequence ^{258}CKEISCVFPEVQ^{269} in SCR4–5 was recognized by the anti-chCR2 mAb (Fig. 4D–G). Notably, it is suitable for IFA (Fig. 4A), WB (Fig. 4B), FCM (Fig. 5A) and IHC (Fig. 6E). As this anti-chCR2 mAb showed limited inhibition of chC3d/chCR2 binding, we assumed that this epitope is not involved in the ligand-binding interaction (data not shown). As our results in the present study show that SCR1–4 are essential for the chCR2–chC3d interaction, we intend to further develop chCR2 mAbs against epitopes from the SCR1–4 region. Collectively, the anti-chCR2 mAb might be a valuable agent for investigation of the functional characteristics of chicken B lymphocytes.

Human CR2 is reportedly mainly expressed on the surface of mature B cells and follicular dendritic cells of immune organs such as lymph nodes and the spleen (14, 46). In this study, quantitative RT-PCR and IHC were used to assess the expression of chCR2 in chicken tissues. The results showed that chCR2 was mainly expressed in the bursa, spleen, thymus, and PBLs rather than nonimmune organs, such as the brain or liver (Fig. 6A–E). Meanwhile, the FCM results indicated that, among the Bu-1 (a commercial Ab against chicken BCR)–positive cells, 98.04% of bursal B lymphocytes and 80.62% of DT40 cells are expressed in the chCR2 protein (Fig. 5A, 5B). These data suggest that chCR2 is mainly expressed in chicken B cells. The differences in expression between CR2 and Bu-1 in DT40 cells was likely due to DT40 being derived from an avian leukosis virus–induced bursal lymphoma that had undergone gene conversion, thus leading to diminished CR2 expression capacity (47). However, 1.83% of bursa lymphocytes and 4.62% of DT40 cells were Bu-1–positive but could not be detected by chCR2-specific mAb, suggesting that some of the B cells in bursa lymphocytes and DT40 cells did not express chCR2. The identity of these cells requires further investigation. Furthermore, CLSM showed that chCR2 colocalized with the cell membrane marker Na,K-ATPase on the membrane of DT40 cells, thus further confirming that chCR2 was mainly expressed on the surface of B cells (Fig. 5C). Nevertheless, our findings illustrate that chCR2 is a surface marker of chickens B cells.

Previous studies have shown that the EBV surface glycoprotein gp350/220 can bind to CR2 to promote viral invasion of host cells (48, 49). However, other studies have shown that during antitumor therapy, a B cell subset is enriched in the tumor microenvironment and CR2-mediated signal transduction causes cell differentiation (42, 50). In addition, HIV binds to dendritic cells and B cells mainly through CR2 binding to C3d-conditioned HIV complexes, in a process known as Ab-dependent enhancement of viral infection (41, 51). IBDV causes a chicken immunosuppressive disease by infecting B lymphocytes in the bursa of Fabricius (52). Our data revealed that chCR2 expression in bursal cells was upregulated by infection with IBDV but downregulated in a dose-dependent manner by immunization with IBDV-inactivated vaccine because IBDV replication was inhibited (Fig. 6F). Furthermore, the expression of chCR2 was significantly increased in DT40 cells infected with IBDV at different points (Fig. 6G). This suggests that chCR2 plays a critical role in the host immune response to the IBDV infection. Moreover, although immature B cells are the predominant target of IBDV infection in bursa, B cell progenitors migrate and rapidly develop into mature B cells to provide an immune response against

infection. Thus, the expression change of chCR2 suggests that migration and maturation of B cells may be induced by stimulation of IBDV infection in bursal follicles, and chCR2 expression possibly drives B cell proliferation, which is distinct from that of mammals. Further research is required to validate this result.

In conclusion, we identified and characterized CR2 in chickens. We hope that the results and mAbs developed in the current study will be useful for further investigations of related functions of chicken B lymphocytes and the chicken immune system.

Acknowledgments

We are indebted to Prof. Xin Guo (College of Veterinary Medicine, China Agricultural University) for valuable comments and suggestions in this manuscript. We thank the Institute of Biophysics, Chinese Academy of Science for our SPR, and we are grateful to Dr. Jing Yang and Bingxue Zhou for help in taking and analyzing SPR images.

Disclosures

The authors have no financial conflicts of interest.

References

1. Bordet, J., and O. Gengou. 1901. Sur l'existence de substances sensibilisatrices dans la plupart des sé rums anti-microbiens. *Ann. Inst. Pasteur (Paris)* 15: 289–302.
2. Chaplin, D. D. 2010. Overview of the immune response. *J. Allergy Clin. Immunol.* 125(2 Suppl 2): S3–S23.
3. Lukácsi, S., B. Mácsik-Valent, Z. Nagy-Baló, K. G. Kovács, K. Kliment, Z. Bajtay, and A. Erdei. 2020. Utilization of complement receptors in immune cell-microbe interaction. *FEBS Lett.* 594: 2695–2713.
4. Roozendaal, R., and M. C. Carroll. 2007. Complement receptors CD21 and CD35 in humoral immunity. *Immunol. Rev.* 219: 157–166.
5. Carroll, M. C. 1998. CD21/CD35 in B cell activation. *Semin. Immunol.* 10: 279–286.
6. Carroll, M. C., and D. E. Isenman. 2012. Regulation of humoral immunity by complement. *Immunity* 37: 199–207.
7. Fischer, M. B., M. Ma, S. Goerg, X. Zhou, J. Xia, O. Finco, S. Han, G. Kelsoe, R. G. Howard, T. L. Rothstein, et al. 1996. Regulation of the B cell response to T-dependent antigens by classical pathway complement. *J. Immunol.* 157: 549–556.
8. Carroll, M. C. 2004. The complement system in B cell regulation. *Mol. Immunol.* 41: 141–146.
9. Carroll, M. C. 2004. The complement system in regulation of adaptive immunity. *Nat. Immunol.* 5: 981–986.
10. Carroll, M. C. 1998. The role of complement and complement receptors in induction and regulation of immunity. *Annu. Rev. Immunol.* 16: 545–568.
11. Hannan, J. P. 2016. The structure-function relationships of complement receptor type 2 (CR2; CD21). *Curr. Protein Pept. Sci.* 17: 463–487.
12. Reynes, M., J. P. Aubert, J. H. Cohen, J. Audouin, V. Tricottet, J. Diebold, and M. D. Kazatchkine. 1985. Human follicular dendritic cells express CR1, CR2, and CR3 complement receptor antigens. *J. Immunol.* 135: 2687–2694.
13. Liu, Y. J., J. Xu, O. de Bouteiller, C. L. Parham, G. Grouard, O. Djossou, B. de Saint-Vis, S. Lebecque, J. Banchereau, and K. W. Moore. 1997. Follicular dendritic cells specifically express the long CR2/CD21 isoform. *J. Exp. Med.* 185: 165–170.
14. Libert, F., and G. Vassart. 1989. Structure-function relationships of the complement components. *Immunol. Today* 10: 407.
15. Guthridge, J. M., J. K. Rakstang, K. A. Young, J. Hinshelwood, M. Aslam, A. Robertson, M. G. Gipson, M. R. Sarrias, W. T. Moore, M. Meagher, et al. 2001. Structural studies in solution of the recombinant N-terminal pair of short consensus/complement repeat domains of complement receptor type 2 (CR2/CD21) and interactions with its ligand C3dg. *Biochemistry* 40: 5931–5941.
16. Hannan, J. P., K. A. Young, J. M. Guthridge, R. Asokan, G. Szakonyi, X. S. Chen, and V. M. Holers. 2005. Mutational analysis of the complement receptor type 2 (CR2/CD21)-C3d interaction reveals a putative charged SCR1 binding site for C3d. *J. Mol. Biol.* 346: 845–858.
17. Delcayre, A. X., F. Salas, S. Mathur, K. Kovats, M. Lotz, and W. Lernhardt. 1991. Epstein Barr virus/complement C3d receptor is an interferon alpha receptor. *EMBO J.* 10: 919–926.
18. Hibbert, R. G., P. Teriete, G. J. Grundy, R. L. Beavil, R. Reljic, V. M. Holers, J. P. Hannan, B. J. Sutton, H. J. Gould, and J. M. McDonnell. 2005. The structure of human CD23 and its interactions with IgE and CD21. *J. Exp. Med.* 202: 751–760.
19. Young, K. A., X. S. Chen, V. M. Holers, and J. P. Hannan. 2007. Isolating the Epstein-Barr virus gp350/220 binding site on complement receptor type 2 (CR2/CD21). *J. Biol. Chem.* 282: 36614–36625.
20. Kovacs, J. M., J. P. Hannan, E. Z. Eisenmesser, and V. M. Holers. 2009. Mapping of the C3d ligand binding site on complement receptor 2 (CR2/CD21) using nuclear magnetic resonance and chemical shift analysis. *J. Biol. Chem.* 284: 9513–9520.
21. Kovacs, J. M., J. P. Hannan, E. Z. Eisenmesser, and V. M. Holers. 2010. Biophysical investigations of complement receptor 2 (CD21 and CR2)-ligand interactions reveal amino acid contacts unique to each receptor-ligand pair. *J. Biol. Chem.* 285: 27251–27258.
22. Moore, M. D., N. R. Cooper, B. F. Tack, and G. R. Nemerow. 1987. Molecular cloning of the cDNA encoding the Epstein-Barr virus/C3d receptor (complement receptor type 2) of human B lymphocytes. *Proc. Natl. Acad. Sci. USA* 84: 9194–9198.
23. Barel, M., M. Balbo, and R. Frade. 1998. Evidence for a new transcript of the Epstein-Barr virus/C3d receptor (CR2, CD21) which is due to alternative exon usage. *Mol. Immunol.* 35: 1025–1031.
24. Schwab, J., and H. Illges. 2001. Regulation of CD21 expression by DNA methylation and histone deacetylation. *Int. Immunol.* 13: 705–710.
25. Schwab, J., and H. Illges. 2001. Silencing of CD21 expression in synovial lymphocytes is independent of methylation of the CD21 promoter CpG island. *Rheumatol. Int.* 20: 133–137.
26. Matsumoto, A. K., J. Kopicky-Burd, R. H. Carter, D. A. Tuveson, T. F. Tedder, and D. T. Fearon. 1991. Intersection of the complement and immune systems: a signal transduction complex of the B lymphocyte-containing complement receptor type 2 and CD19. *J. Exp. Med.* 173: 55–64.
27. Engel, P., L. J. Zhou, D. C. Ord, S. Sato, B. Koller, and T. F. Tedder. 1995. Abnormal B lymphocyte development, activation, and differentiation in mice that lack or overexpress the CD19 signal transduction molecule. *Immunity* 3: 39–50.
28. Kieslich, C. A., and D. Morikis. 2012. The two sides of complement C3d: evolution of electrostatics in a link between innate and adaptive immunity. *PLOS Comput. Biol.* 8: e1002840.
29. Levy, S., S. C. Todd, and H. T. Maecker. 1998. CD81 (TAPA-1): a molecule involved in signal transduction and cell adhesion in the immune system. *Annu. Rev. Immunol.* 16: 89–109.
30. Tedder, T. F., K. M. Haas, and J. C. Poe. 2002. CD19-CD21 complex regulates an intrinsic Src family kinase amplification loop that links innate immunity with B-lymphocyte intracellular calcium responses. *Biochem. Soc. Trans.* 30: 807–811.
31. Tedder, T. F., M. Inaoki, and S. Sato. 1997. The CD19-CD21 complex regulates signal transduction thresholds governing humoral immunity and autoimmunity. *Immunity* 6: 107–118.
32. Tedder, T. F., J. C. Poe, M. Fujimoto, K. M. Haas, and S. Sato. 2005. The CD19-CD21 signal transduction complex of B lymphocytes regulates the balance between health and autoimmune disease: systemic sclerosis as a model system. *Curr. Dir. Autoimmun.* 8: 55–90.
33. Shoham, T., R. Rajapaksa, C. Boucheix, E. Rubinstein, J. C. Poe, T. F. Tedder, and S. Levy. 2003. The tetraspanin CD81 regulates the expression of CD19 during B cell development in a postendoplasmic reticulum compartment. *J. Immunol.* 171: 4062–4072.
34. Jin, H., Z. Kong, A. Mehboob, B. Jiang, J. Xu, Y. Cai, W. Liu, J. Hong, and Y. Li. 2020. Transcriptional profiles associated with Marek's disease virus in bursa and spleen lymphocytes reveal contrasting immune responses during early cytolytic infection. *Viruses* 12: 354.
35. Jiang, N., H. Jin, Y. Li, X. Ge, J. Han, X. Guo, L. Zhou, and H. Yang. 2017. Identification of a novel linear B-cell epitope in nonstructural protein 11 of porcine reproductive and respiratory syndrome virus that are conserved in both genotypes. *PLoS One* 12: e0188946.
36. Zhang, X., D. Fei, L. Sun, M. Li, Y. Ma, C. Wang, S. Huang, and M. Ma. 2019. Identification of the novel host protein interacting with the structural protein VP1 of Chinese sacbrood virus by yeast two-hybrid screening. *Front. Microbiol.* 10: 2192.
37. Dalgaard, T., M. K. Boving, K. Handberg, K. H. Jensen, L. R. Norup, and H. R. Juul-Madsen. 2009. MHC expression on spleen lymphocyte subsets in genetically resistant and susceptible chickens infected with Marek's disease virus. *Viral Immunol.* 22: 321–327.
38. Vu Manh, T. P., H. Marty, P. Sibille, Y. Le Vern, B. Kaspers, M. Dalod, I. Schwartz-Cornil, and P. Quéré. 2014. Existence of conventional dendritic cells in *Gallus gallus* revealed by comparative gene expression profiling. *J. Immunol.* 192: 4510–4517.
39. Dash, R., and N. Das. 2017. Complement receptor 2 (CR2/CD21). *Int. J. Res. Med. Sci.* 5: 1156–1160.
40. Herrero, R., L. M. Real, A. Rivero-Juárez, J. A. Pineda, Á. Camacho, J. Macías, M. Laplana, P. Konieczny, F. J. Márquez, J. C. Souto, et al. 2015. Association of complement receptor 2 polymorphisms with innate resistance to HIV-1 infection. *Genes Immun.* 16: 134–141.
41. Meza, G., A. Expósito, J. L. Royo, C. Ruiz-García, B. Sánchez-Arcas, F. J. Marquez, M. A. Gómez-Vidal, M. Omar, F. Sinangil, K. Higgins, et al. 2020. Association of complement C3d receptor 2 genotypes with the acquisition of HIV infection in a trial of recombinant glycoprotein 120 vaccine. *AIDS* 34: 25–32.
42. Lu, Y., Q. Zhao, J. Y. Liao, E. Song, Q. Xia, J. Pan, Y. Li, J. Li, B. Zhou, Y. Ye, et al. 2020. Complement signals determine opposite effects of B cells in chemotherapy-induced immunity. *Cell* 180: 1081–1097.e24.
43. Pringle, E. S., M. A. Firth, K. S. Chattha, D. C. Hodgins, and P. E. Shewen. 2012. Expression of complement receptors 1 (CR1/CD35) and 2 (CR2/CD21), and co-signaling molecule CD19 in cattle. *Dev. Comp. Immunol.* 38: 487–494.
44. Donius, L. R., and J. H. Weis. 2014. Detection of complement receptors 1 and 2 on mouse splenic B cells using flow cytometry. *Methods Mol. Biol.* 1100: 305–310.

45. Jiang, B., Z. Zhang, J. Xu, H. Jin, Tuya, and Y. Li. 2021. Cloning and structural analysis of complement component 3d in wild birds provides insight into its functional evolution. *Dev. Comp. Immunol.* 117: 103979.
46. Fagerberg, L., B. M. Hallström, P. Oksvold, C. Kampf, D. Djureinovic, J. Odeberg, M. Habuka, S. Tahmasebpoor, A. Danielsson, K. Edlund, et al. 2014. Analysis of the human tissue-specific expression by genome-wide integration of transcriptomics and antibody-based proteomics. *Mol. Cell. Proteomics* 13: 397–406.
47. Winding, P., and M. W. Berchtold. 2001. The chicken B cell line DT40: a novel tool for gene disruption experiments. *J. Immunol. Methods* 249: 1–16.
48. Jog, N. R., K. A. Young, M. E. Munroe, M. T. Harmon, J. M. Guthridge, J. A. Kelly, D. L. Kamen, G. S. Gilkeson, M. H. Weisman, D. R. Karp, et al. 2019. Association of Epstein-Barr virus serological reactivation with transitioning to systemic lupus erythematosus in at-risk individuals. *Ann. Rheum. Dis.* 78: 1235–1241.
49. Young, K. A., A. P. Herbert, P. N. Barlow, V. M. Holers, and J. P. Hannan. 2008. Molecular basis of the interaction between complement receptor type 2 (CR2/CD21) and Epstein-Barr virus glycoprotein gp350. *J. Virol.* 82: 11217–11227.
50. van der Poel, C. E., and M. C. Carroll. 2017. Untangling Fc and complement receptors to kill tumors. *Nat. Immunol.* 18: 874–875.
51. Kacani, L., W. M. Prodinger, G. M. Sprinzl, M. G. Schwendinger, M. Spruth, H. Stoiber, S. Döpper, S. Steinhuber, F. Steindl, and M. P. Dierich. 2000. Detachment of human immunodeficiency virus type 1 from germinal centers by blocking complement receptor type 2. *J. Virol.* 74: 7997–8002.
52. Mahgoub, H. A., M. Bailey, and P. Kaiser. 2012. An overview of infectious bursal disease. [Published erratum appears in 2012 *Arch. Virol.* 157: 2059.] *Arch. Virol.* 157: 2047–2057.